Progress In Electromagnetics Research C, Vol. 112, 11–20, 2021

Dual-Band Subharmonic Mixer for WIFI Application with Improved Conversion Loss and RF-to-IF Isolation

Kumari Pushpa* **and Jayanta Ghosh**

Abstract—A dual-band subharmonic mixer that employs both the second and fourth harmonics of a local oscillator signal in the mixing process is demonstrated for WIFI application. The design results in a simple and cost-effective mixer as it requires only one local oscillator (LO). A quarter-wave stepped impedance stub has been used to suppress both bands of radio frequency (RF) signal. The proposed dual-band subharmonic mixer is designed for two RF bands with the center frequencies at 2.45 GHz and 5 GHz using a single LO frequency at 1.3 GHz. For mixing purpose, the second and fourth harmonics of LO are utilized. Experimental measurements show high port-to-port isolation and achieve minimum conversion losses of 6.87 dB and 10.0 dB at 2.59 GHz and 5 GHz, respectively. The 3-dB RF bandwidth is 2.3 to 2.95 GHz for the second harmonic and 4.8 to 5.5 GHz for the fourth harmonic of LO signal. The input P1-dB compression points for two modes of the mixer are −9 dBm and −5 dBm, respectively. The RF-to-IF isolations are more than 18 dB (maximum 36 dB) and 20 dB (maximum 33 dB), over both the RF bands.

1. INTRODUCTION

The development of wireless communication, remote sensing, and radar demands low cost and low power RF circuit and transceiver. This leads to the evolution of multiband operation on a single chip [1–4]. Conventionally, multiple single-band transceiver circuits are connected in parallel for multi-band operations, which results in high implementation cost and a large chip area. To remove the above-mentioned drawback, multiband circuits have been demonstrated for multiband applications [5, 6]. For any transceiver, a mixer is a key component. It could be active or passive. The passive mixer is more popular as it is easy to design without any DC power requirement. Further, a mixer can be fundamental or subharmonic. A fundamental mixer uses a local oscillator (LO) signal while a subharmonic mixer (SHM) uses harmonics of LO signal for mixing purposes. At the high frequency range, the unavailability of high power LO source makes SHM a good choice [7–9]. Various multi-band receivers based on impedance matching have been developed [10–12], which require multiple fundamental SHMs. Such an SHM makes the circuit more costly and bulky as it requires a separate LO source for each SHM. Multiband performance can also be achieved by mixing higher-order harmonics of LO signal. Using harmonics, several dual-band SHMs have been developed in the microwave and millimeter-wave range [13–16] using a single diode. However, the main problem with this structure is its poor LO AM noise and LO-to-RF isolations. To overcome such a problem, an antiparallel diode-based SHM has been developed [17] with good port isolations and noise reduction at the cost of conversion loss.

In this paper, a new dual-band mixer architecture is proposed for the WIFI application. This dual-band operation is achieved by usefully exploiting the second and fourth harmonic signal of LO signal generated by antiparallel diode pair (APDP). The operating radio frequency (RF) band can be selected by only tuning the LO power (P_{LO}). Therefore, the bandwidth of the LO does not need to be

Received 4 March 2021, Accepted 7 April 2021, Scheduled 11 April 2021
* Corresponding author: Kumari Pushpa (pushpa.pushpa011@gmail.com).
The authors are with the National Institute of Technology Patna, Ashok Rajpath, Patna, Bihar 800005, India.

wide to cover the two different RF bands. The single LO frequency utilization for two RF bands leads to a simpler structure with high efficiency. In the present design, the RF and intermediate frequency (IF) ports lie on the same side of APDP. The chance of RF leakage to IF side is more. For proper mixing, RF must be blocked on the IF side. To suppress the dual-band RF on the IF side, a stepped impedance stub is used which results in high RF to IF port isolation.

2. MIXER ARCHITECTURE

The proposed mixer topology based on APDP hybrid MIC is shown in Fig. 1. It consists of an APDP, a LO section, an RF section with one high pass filter, and an IF section with an RF blocking section. To reduce the circuit size, the stubs are meandered. The operating frequency of designed mixer is from 2.3 to 2.95 GHz and 4.8 to 5.5 GHz with fixed LO tuned to 1.3 GHz. Accordingly, IF varies from 0 to 400 MHz. For the implementation of this dual-band mixer, Roger 4050B substrate of thickness 0.5 mm with permittivity = 3.66 and loss tangent = 0.0031 is used. For frequency mixing purposes GaAs Schottky APDP is used.

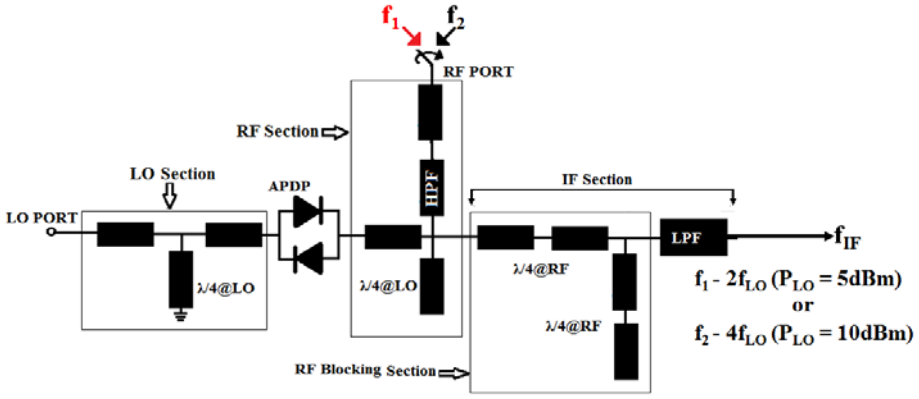

Figure 1. An architecture of the proposed dual-band SHM.

2.1. APDP Schottky Diode

The design of the passive mixer starts with the selection of a nonlinear device. A Schottky anti-parallel diode pair from MACOM with part number MA4E1318 is selected, whose electrical parameter is mentioned in Table 1. To design an optimum mixer circuit, the diode embedding impedance should be matched. It varies with the variation of power and frequency. In the case of the mixer, it is the LO power that is responsible for impedance variation of the diode as it switches the diode on/off. Therefore, for a given diode and frequency it is required to find an optimal value of LO power at which the conversion loss is minimum. The graph for conversion loss (CL) vs LO power is plotted in Fig. 2 where the minimum CL point is point of the optimum LO power. For this dual-band structure, there are two optimum values of LO power for two different RF bands. The optimum LO power is 5 dBm

Table 1. Schottky APDP (MA4E1318) electrical parameters.

Reverse Saturation Current I_s (A)	Series Resistance R_s (Ω)	Ideal Factor N	Zero biased Junction Capacitance C_{j0} (pF)	Reverse Breakdown Voltage B_v (V)	Energy Band Gap E_g (eV)	Built-in Voltage (eV)
1.7×10^{-14}	4.6	1.08	0.047	7	1.43	0.86

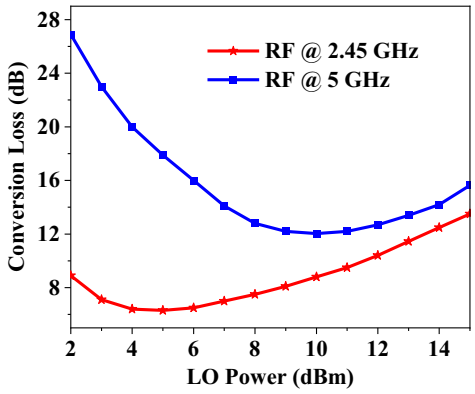

Figure 2. Variation of conversion loss with LO power for an ideal mixer.

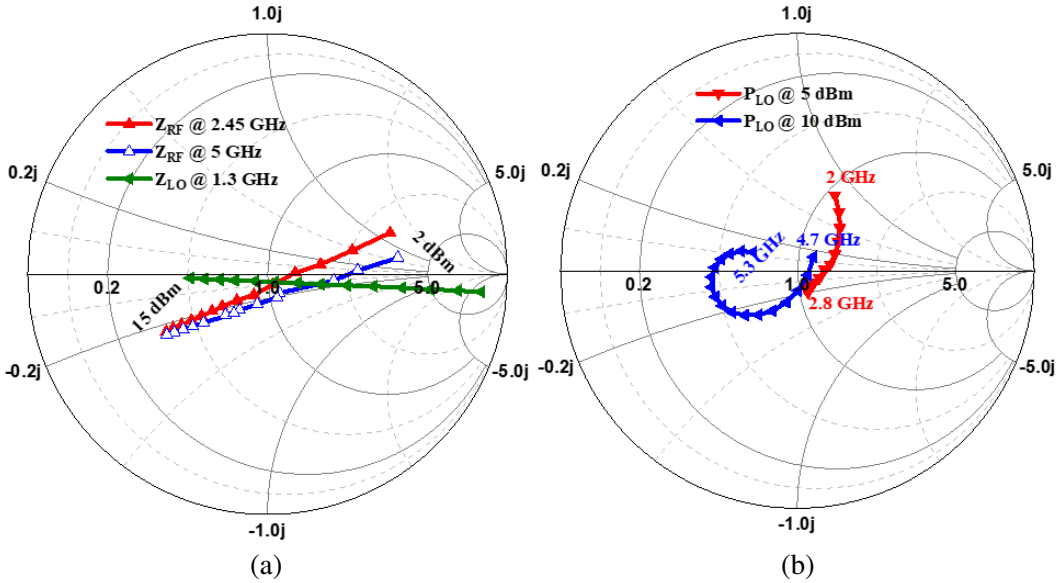

Figure 3. Variation of embedding impedance of diode. (a) With LO power for different frequencies, and (b) with RF frequency for different LO powers.

and 10 dBm for 2.45 GHz and 5 GHz, respectively. At these LO power levels, two sets of impedances are calculated by commercial software [18]. In Fig. 3, the diode embedding impedances for different LO powers and different RF frequencies are plotted. In Fig. 3(a), the graph for embedding impedance of APDP vs LO power for $f_{\mathrm{RF1}} = 2.45$, $f_{\mathrm{RF2}} = 5$ GHz and LO frequency $f_{\mathrm{LO}} = 1.3$ GHz is plotted on the Smith chart. The LO power varies from 2 dBm to 15 dBm for each frequency. Graphical analysis shows that in the lower frequency the real conductance of diode impedance dominates while moving to higher frequency its junction capacitance increases. The change of RF embedding impedance for optimum P_{LO} of 5 dBm and 10 dBm is shown in Fig. 3(b) for both the RF bands. From these graphs, the embedding impedance of the diode is taken for optimum conversion loss of the mixer.

2.2. Working Principle of Dual Band Isolation Circuit

In the proposed structure, RF and IF ports are on the same side of the diode. So, the RF signal can easily leak through the IF port and deteriorates the performance of the mixer. In a single band mixer, this problem is solved by using a quarter wavelength ($\lambda_g/4$) open-stub transmission line (quarter-wave resonator) at RF frequency to block the RF signal. In the present case for the dual-band structure, a

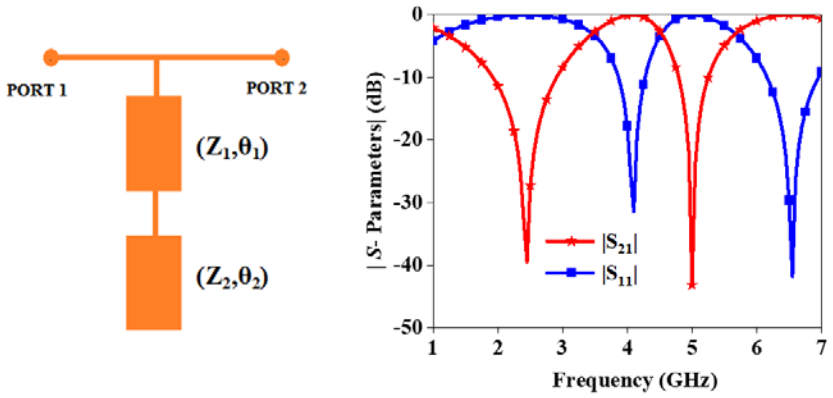

(a) (b)

Figure 4. Stepped impedance, (a) layout and (b) simulated results.

stepped impedance quarter wavelength open-stub transmission line has been used to block two different RF frequencies as shown in Fig. 4(a). The input impedance of such a stepped impedance stub is written as [19]

$$Z_{in} = j\frac{Z_1(Z_1 \tan\theta_1 - Z_2 \cot\theta_2)}{Z_1 + Z_2 \tan\theta_1 \cot\theta_2} \tag{1}$$

where Z_1, Z_2 are characteristic impedances, and θ_1, θ_2 are the electrical lengths of the stepped impedance sections at f_{RF1} and f_{RF2}, respectively. By solving Equation (1) for $Z_{in} = 0$ at f_{RF1} and f_{RF2}, transmission zeroes will be obtained. The obtained electrical parameters for the current design are as $Z_1 = 22.74\,\Omega$, $Z_2 = 86.4\,\Omega$, $\theta_1 = 74.4°$, and $\theta_2 = 47.96°$ at f_{RF1}. Fig. 4(b) shows the simulated S-parameters of the stepped impedance stub. It can be noted that the insertion loss is better than -40 dB for both the RF bands. Hence, it can improve the RF-to-IF isolations for both RF bands.

2.3. LO Section

The LO section is shown in Fig. 5(a). It consists of a simple 50 Ohm transmission line along with a quarter wavelength short-stub at 1.3 GHz. The function of this stub is to increase the isolation of the RF signal without disturbing the LO signal. In the LO section, the impedance at APDP port (port 2) is not fixed to 50 Ohm. It varies as it is directly connected to the APDP. Since LO frequency is fixed to 1.3 GHz, it varies only with LO power (P_{LO}) as shown in Fig. 3(a). In this Smith chart plot, the nearest point to 50 Ohm for 1.3 GHz is $53.33 - j3.5\,\Omega$. P_{LO} at this point is 10 dBm. This power level is

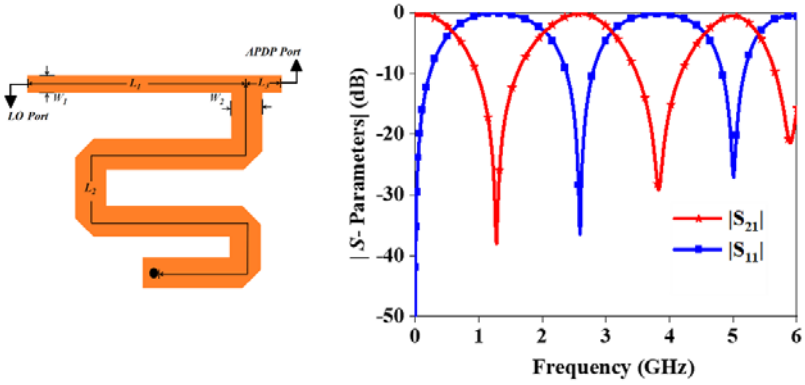

(a) (b)

Figure 5. LO section, (a) layout and (b) simulated results. $L_1 = 14.1$, $L_2 = 34.3$, $L_3 = 2.2$, $W_1 = 1.13$, $W_2 = 2$. All dimensions are in mm.

selected so that the design of the LO section at this power level does not require any matching section for APDP. The simulation for S-parameters of the LO section is shown in Fig. 5(b) where both RF signals are suppressed by at least 28 dB. Moreover, it also gives return path to the IF signal.

2.4. RF Section

RF section consists of an APDP matching section, one high pass filter, and a quarter wavelength open-stub at 1.3 GHz. The layout of designed RF section is shown in Fig. 6(a). For dual-band operation, there are two sets of embedding impedance of APDP which is shown in Fig. 3(b). The embedding impedances (Z_L) seen at RF APDP port (port 2) is $60 + j3.7\,\Omega$ at 2.45 GHz and $30 + j12.2\,\Omega$ at 5 GHz for LO powers of 5 dBm and 10 dBm, respectively. As the imaginary part of Z_L is low for both the RF bands, this impedance can be matched to a 50 Ohm transmission line using a single stub. Here a single stub of length L_4 is used for matching purposes. As discussed above, it is possible that the IF signal generated by APDP leaks through the RF port and finally radiates through the antenna. So, it is necessary to block the IF signal on the RF side. For this purpose, one high pass filter is designed using one narrow line shorted stub of length L_2 and a series capacitor of value 3.5 pF. Also, for LO rejection on the RF side of the diode one-quarter wavelength, an open stub at 1.3 GHz has been used. It suppresses the LO signal but acts as an open circuit for RF signals. The S parameters simulation of the designed RF section with $Z_L = 60 + j3.7\,\Omega$ at RF APDP port is shown in Fig. 6(b). It shows the suppression of IF and LO signal more than 20 dB and transmission of the second harmonic band with a minimum insertion loss of 0.43 dB at 2.45 GHz. For the fourth harmonic band, the S parameters simulation with $Z_L = 30 + j12.2\,\Omega$ is shown in Fig. 6(c). In this case also the suppression of IF and LO signal is more than 30 dB.

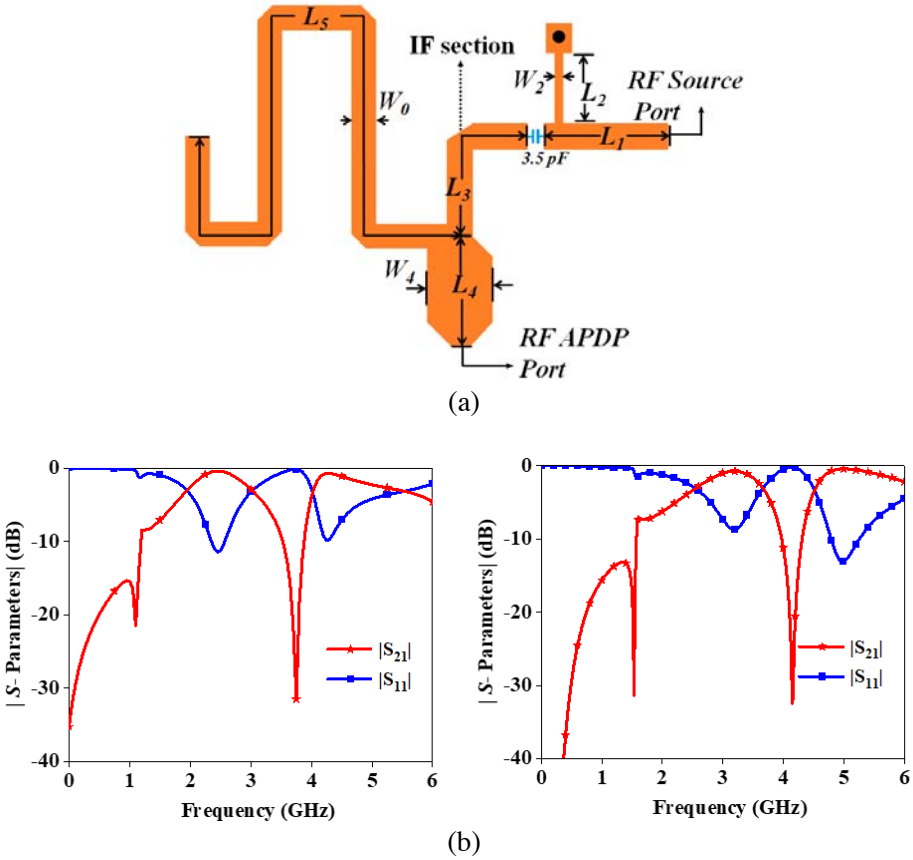

Figure 6. RF section, (a) layout and (b) simulated results for $Z_L = 60 + j3.7\,\Omega$ and (c) simulated S parameters results for $Z_L = 30 + j12.2\,\Omega$. $L_1 = 5.7$, $L_2 = 3.8$, $L_3 = 7.9$, $L_4 = 5$, $L_5 = 36.2$, $W_0 = 1.13$, $W_2 = 0.4$, $W_4 = 3$. All dimensions are in mm.

2.5. IF Section

One of the drawbacks of SHM is the leakage of signals from one port to another. Similar to RF and LO sections, here also LO and RF signals can pass through the IF port. So, this also requires LO and RF blocking sections. The design of stepped impedance, i.e., previously discussed in Section 2.1, is used for RF blocking section. LO signal is suppressed by the same stub, i.e., used in the RF section as RF and IF are on the same side of APDP. The layout of the IF section is shown in Fig. 7(a). It consists of the stepped impendence section along with one shunt capacitor of value 0.1 pF. This capacitor is used to filter out all unwanted harmonics, so that the signal obtained at IF frequency will be spurious-free. The IF output is calculated at port 1, and port 2 is connected to RF section. The S-parameters simulation in Fig. 7(b) shows two transmission zeroes at 2.45 GHz and 5 GHz along with passband at low frequency.

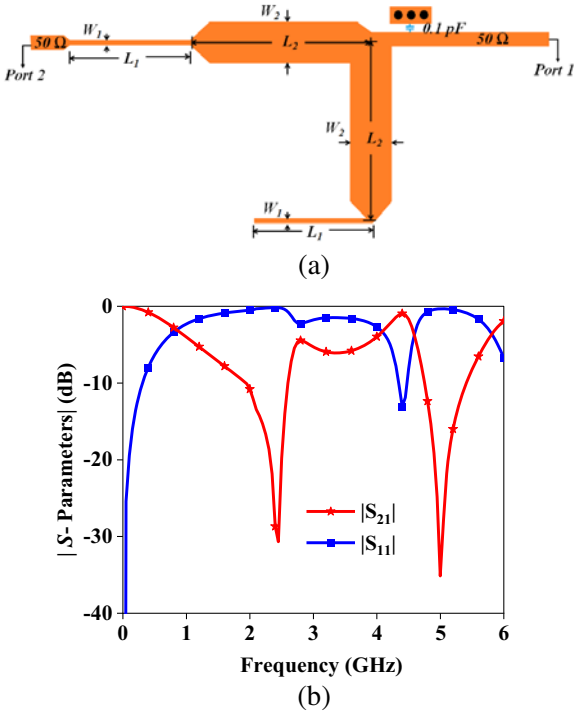

Figure 7. IF sections, (a) layout and (b) simulated S-parameters results. $L_1 = 9.8$, $L_2 = 4.7$, $W_1 = 0.4$, $W_2 = 2.5$. All dimensions are in mm.

After designing all three networks successfully, they are combined all together to complete the mixer circuit. After that, nonlinear analysis is performed on this whole structure to calculate the conversion loss, isolations, and P1 dB compression point of the mixer.

3. EXPERIMENTAL ANALYSIS

The designed mixer is fabricated on the above-mentioned substrate. A photograph of the fabricated dual-band mixer is shown in Fig. 8(a). It is designed to convert two RF bands around 2.45 GHz and 5 GHz using a single LO. As in an APDP type diode, its second and fourth harmonics are used for mixing with the RF band. The performance parameters of the mixer are measured using SMC signal generators from Rohde & Schwarz, an Agilent E8257D PSG signal generator, and an Agilent N9020A MXA Signal Analyzer. For all measurements, RF power is kept fixed at −30 dBm. The measured CL performance for both RF bands is shown in Fig. 8(b). The measured conversion losses in both the RF bands show good agreement with the simulated conversion loss. The graph of RF-to-IF isolation is shown in Fig. 9. The maximum RF-to-IF isolations are 36 dB and 33 dB at 2.45 GHz and 5 GHz, respectively. The highest

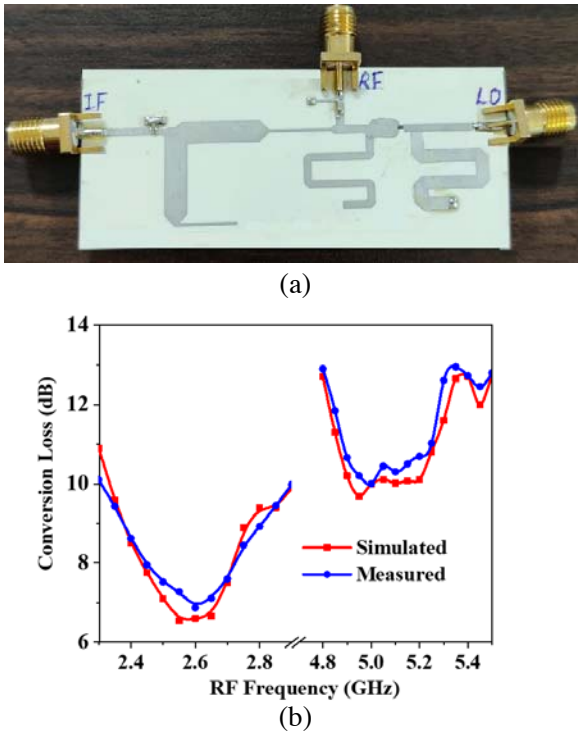

Figure 8. (a) Photograph of the fabricated dual-band mixer, and (b) measured down-conversion loss versus RF frequency.

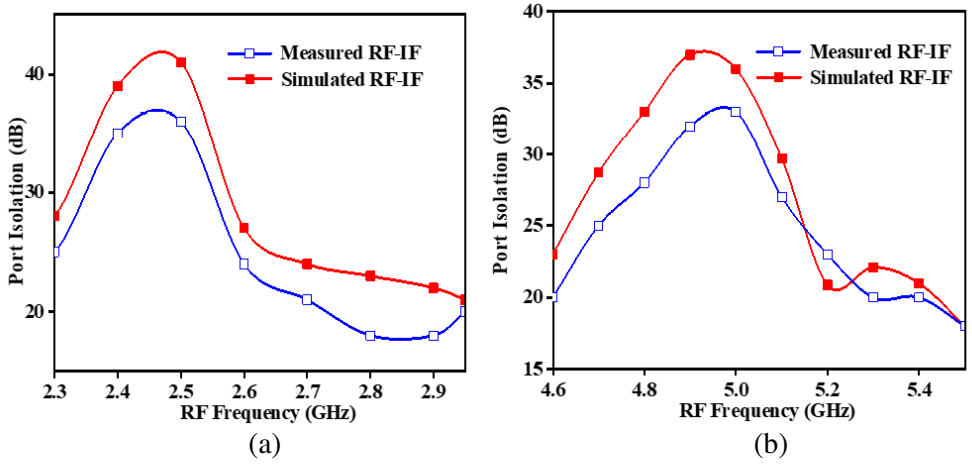

Figure 9. RF-to-IF isolation, (a) second harmonic, and (b) fourth harmonic.

insertion loss of the quarter-wave stepped impedance stub at these frequencies results in maximum RF-to-IF isolation at these points. The measured LO-to-RF, 2LO-to-RF, and LO-to-IF isolations are better than 41 dB, 46 dB, and 46.9 dB, respectively, for both RF bands. The graph for IP1 dB compression point is shown in Fig. 10, where the measured data are almost same as the simulated one. The measured P1 dB is -9 dB and -5 dBm at 2.45 and 5 GHz, respectively. Table 2 compares some recent dual-band mixers based on single and double LO sources. Despite using the fourth harmonic of LO, the conversion loss of this mixer is comparable to other mixers. Compared to the previous APDP-based mixers, this mixer also has good isolation and noise cancellation.

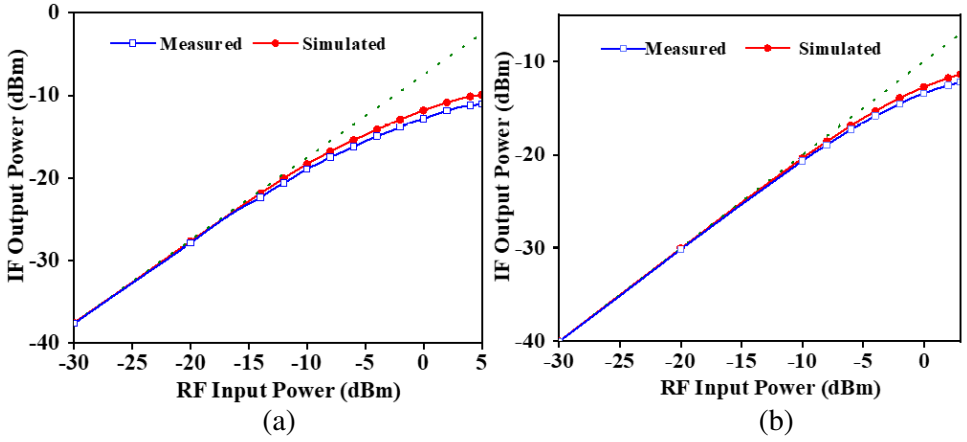

Figure 10. P1 dB compression point, (a) second harmonic, and (b) fourth harmonic.

Table 2. Comparison of dual-band mixers.

Reference	[12]	[14]	[15]	[17]	[20]	[21]	**Present Work**
Technology	Hybrid MIC	Hybrid MIC	CMOS	Hybrid MIC	Hybrid MIC	Hybrid MIC	Hybrid MIC
Frequency (GHz)	1.7–1.9/2.5–2.7	1/3	5–6/9.8–11.8	2.4/5	2.41/3.61	26.5–40	2.3–2.95/4.8–5.5
Bandwidth (GHz)	0.4	-	3	-	-	13.5	1.35
Harmonic Number	1	1	1 and 2	2/4	2/3	4	2/4
P_{LO} (dBm)	0	4	0	4	0	11	5/10
V_{DC} (mW)	0	0	1.5	0	0.25/0.53	0	0
Conversion Loss (dB)	15/10	15/16	5–12	11.14/12.72	8.1/8.9	6.1–16	6.87–12.9
IP_{dB} (dBm)	$-3/-6$	-	>-5	-	-	-	$-9/-5$
Dual-Band	Yes	Yes	Yes	Yes	Yes	NO	Yes
Area (mm^2)	-	55.22×44	0.525	-	-	-	67.5×27.5

4. CONCLUSIONS

A new topology of a dual-band subharmonic mixer with a single LO frequency has been designed, simulated, and fabricated. We have used to design the mixer by interpreting optimum LO power that minimizes the conversion loss at each band. The open stepped impedance stub has been used to improve this RF to IF isolation for both the RF bands. The proposed dual-band SHM is demonstrated at RF bands of 2.3 to 2.95 GHz and 4.8 to 5.5 GHz with single LO at 1.3 GHz. Only varying the LO power, it shows the minimum CLs of 6.87 dB and 10 dB at 2.59 GHz and 5 GHz, respectively. The measured IP1 dB is -9 dB and -5 dBm at 2.45 and 5 GHz, respectively. The 1 dB compression point of the present mixer is low as it is designed with low turn on diode in antiparallel configuration without any DC bias. As this dual-band mixer operates with only one LO source without any DC biasing, it results in reduced system complexity and reduced power consumption. This technique could also be attractive at the millimeter-wave frequency where frequency multiplier is used in front of LO.

REFERENCES

1. Zheng, X., Y. Liu, C. Yu, S. Li, and J. Li, "Design of a dual-band Doherty power amplifier utilizing simplified phase offset-lines," *Progress In Electromagnetics Research C*, Vol. 48, 21–28, 2014.
2. Wolf, R., N. Joram, S. Schumann, and F. Ellinger, "Dual-band impedance transformation networks for integrated power amplifiers," *Int. J. Microw. Wirel. Technol.*, Vol. 8, No. 1, 1–7, 2016, doi: 10.1017/S1759078714001391.
3. Zaidi, A. M., S. A. Imam, B. Kanaujia, and K. Rambabu, "A new equal power quadrature branch line coupler for dual-band applications," *Progress In Electromagnetics Research Letters*, Vol. 74, 61–67, 2018.
4. Lv, G., W. Chen, X. Chen, and Z. Feng, "An energy-efficient K a/Q dual-band power amplifier MMIC in 0.1-μm GaAs process," *IEEE Microw. Wirel. Components Lett.*, Vol. 28, No. 6, 530–532, 2018, doi: 10.1109/LMWC.2018.2832841.
5. Eldek, A., A. Elsherbeni, and C. Smith, "Dual-wideband square slot antenna with a U-shaped printed tuning stub for personal wireless communication systems," *Progress In Electromagnetics Research*, Vol. 53, 319–333, 2005.
6. Jain, V., F. Tzeng, L. Zhou, and P. Heydari, "A single-chip dual-band 22–29-GHz/77–81-GHz BiCMOS transceiver for automotive radars," *IEEE Journal of Solid-State Circuits*, Vol. 44, No. 12, 3469–3485, 2009, doi: 10.1109/JSSC.2009.2032583.
7. Cohn, M., J. E. Degenford, and B. A. Newman, "Harmonic mixing with an antiparallel diode pair," *IEEE Trans. Microw. Theory Tech.*, Vol. 23, No. 8, 667–673, 1975, doi: 10.1109/TMTT.1975.1128646.
8. Yum, T. Y., Q. Xue, and C. H. Chan, "Novel subharmonically pumped mixer incorporating dual-band stub and in-line SCMRC," *IEEE Trans. Microw. Theory Tech.*, Vol. 51, No. 12, 2538–2547, 2003, doi: 10.1109/TMTT.2003.820152.
9. Kumari, S., R. Pal, and P. Mondal, "A wideband subharmonic mixer with low conversion loss and high port-to-port isolations," *IEEE Trans. Circuits Syst. II: Express Briefs*, Vol. 67, No. 10, 1695–1699, 2019, doi: 10.1109/tcsii.2019.2943749.
10. Hwang, Y. S., S. S. Yoo, and H. J. Yoo, "A 2 GHz and 5 GHz dual-band direct conversion RF front-end for multi-standard applications," *Proc. — IEEE Int. SOC Conf.*, 189–192, 2005, doi: 10.1109/socc.2005.1554492.
11. Liang, C. P., P. Z. Rao, T. J. Huang, and S. J. Chung, "A 2.45/5.2 GHz image rejection mixer with new dual-band active notch filter," *IEEE Microw. Wirel. Components Lett.*, Vol. 19, No. 11, 716–718, 2009, doi: 10.1109/LMWC.2009.2032013.
12. Ning, Z., Y. Liu, Y. Wu, and J. Yu, "A novel dual-band mixer using arbitrary impedances-matching coupler for long-term evolution applications," *Electromagnetics*, Vol. 35, No. 3, 205–215, 2015, doi: 10.1080/02726343.2015.1005277.
13. De Paco, P., R. Villarino, G. Junkin, Ó. Menéndez, E. Corrales, and J. Parrón, "Dual-band mixer using composite right/left-handed transmission lines," *IEEE Microw. Wirel. Components Lett.*, Vol. 17, No. 8, 607–609, 2007, doi: 10.1109/LMWC.2007.901788.
14. Lin, I. H., K. M. K. H. Leong, C. Caloz, and T. Itoh, "Dual-band sub-harmonic quadrature mixer using composite right/left-handed transmission lines," *IEE Proc. Microwaves, Antennas Propag.*, Vol. 153, No. 4, 365–375, 2006, doi: 10.1049/ip-map:20050138.
15. Jackson, B. R. and C. E. Saavedra, "A dual-band self-oscillating mixer for C-band and X-band applications," *IEEE Trans. Microw. Theory Tech.*, Vol. 58, No. 2, 318–323, 2010.
16. Zhu, F. and G. Q. Luo, "A millimeter-wave fundamental and subharmonic hybrid CMOS mixer for dual-band applications," *Int. J. Microw. Wirel. Technol.*, 1–6, 2020, doi: 10.1017/S1759078720001270.
17. Pushpa, K., P. Mondal, and A. Singh, "A dual-band subharmonic mixer with high RF-IF isolation," *2017 Progress In Electromagnetics Research Symposium — Fall (PIERS — FALL)*, 1183–1189, Singapore, Nov. 19–22, 2017.
18. Advanced Design System, Keysight Technologies, Santa Rosa, CA, USA, 2015.

19. Sagawa, M., M. Makimoto, and S. Yamashita, "Geometrical structures and fundamental characteristics of microwave stepped-impedance resonators," *IEEE Trans. Microw. Theory Tech.*, Vol. 45, No. 7, 1078–1085, 1997, doi: 10.1109/22.598444.
20. Perhirin, S. and Y. Auffret, "A dual-band subharmonic drain mixer based on single local oscillator," *Microw. Opt. Technol. Lett.*, Vol. 55, No. 11, 2562–2568, 2013, doi: 10.1002/mop.
21. Xue, Q., K. M. Shum, and C. H. Chan, "Low conversion-loss fourth subharmonic mixers incorporating CMRC for millimeter-wave applications," *IEEE Trans. Microw. Theory Tech.*, Vol. 51, No. 5, 1449–1454, 2003, doi: 10.1109/TMTT.2003.810153.